

## Phase behavior in binary and ternary water–salt systems at high temperatures and pressures

Vladimir M. Valyashko

*Kurnakov Institute of General and Inorganic Chemistry,  
Russian Academy of Sciences, Moscow 117907, Russia*

*Abstract:* In the present review some selected results on liquid-liquid immiscibility, salt solubility, critical and tricritical phenomena in hydrothermal systems are presented. The data on phase behavior of water - salt mixtures have been obtained in a frame of approach to systematic investigation of phase equilibria over a wide range of parameters discussed earlier in this Journal (Pure & Appl.Chem. 67, 567 (1995).

Water-salt mixtures belong to a large class of systems characterized by different volatility of the components. Water is always the volatile component, whereas nonvolatile components are inorganic compounds with low vapor pressure and high melting temperature (often higher than critical temperature of water).

Main regularities of phase behavior in binary and ternary systems over a wide range of temperatures and pressures can be represented by means of complete phase diagrams. The diagrams describe all equilibria with gas (vapor), liquid and/or solid phases in a wide range of parameters and useful for systems with the components of different volatility, whether they are hydrocarbons, water, inorganic gases or salts.

In preceding reviews [1-3] the fundamental idea of continuous transitions between fluid phase diagrams, originally formulated by G.M.Schneider [4], was applied to complete phase diagrams, and the method of continuous topological transformation of complete phase diagrams was developed. This method permits not only to accumulate of available experimental data on phase equilibria and to obtain the systematic classification of binary mixtures, but also derivation of new versions of phase diagram for binary and ternary systems. The combination of experimental studies with theoretical derivation of topological schemes for the phase diagrams establish a new approach to systematic investigation of water-salt equilibria in a wide range of temperatures and pressures.

The present review considers some recent results on hydrothermal phase equilibria, concentrating on tricritical phenomena, and thermodynamic calculation of solubility in ternary water-salt systems. We have been obtained data using the new approach mentioned above.

### BINARY SYSTEMS

Two main types of hydrothermal systems or systems with solid-supercritical phase equilibria, can be distinguished according to the nature of P-T projections of their phase diagrams. Particularly, the types of system is distinguished by the presence or absence of the intersection of the critical curve (L=G) and the three-phase solubility curve (L-G-S) [1-6].

The first type of the system (water-salt systems, or salts in water-salt mixtures) is distinguished by the absence of an intersection of the critical and solubility curves. That implies the lack of critical phenomena between liquid and gas (vapour) in the solutions saturated with the solid (L=G-S). The salt solubility in the three-phase equilibrium L-G-S increases with increasing temperature (positive

temperature coefficient of solubility (t.c.s.) up to the melting temperature of the salt component. The three-phase solubility curve has a maximum of vapor pressure. The water-salt systems whose salt components are, so called, "high solubility" compounds such as NaOH, KOH, NaCl, KCl,  $\text{Na}_2\text{B}_4\text{O}_7$ ,  $\text{PbBr}_2$ ,  $\text{HgI}_2$  etc. usually belong to this type of system.

Figure 1a shows the critical curves L=G of the first type of water-salt systems. The curves start in the critical point of water and end in the critical point of salt component without intersection by the solubility curves.

In systems of the second (p-Q) type, increasing temperature corresponds to a decrease in solubility of the salt in the subcritical area (negative t.c.s). This results in an increasingly similar composition of saturated liquid and vapour. At temperatures above the critical temperature of water, critical phenomena are observed in saturated solutions. The first critical end point ("p" (L=G-S)) is the intersection of the critical and the solubility curves. The second critical end point Q occurs at higher temperatures, pressures and salt concentrations. The supercritical fluid equilibria exist in a temperature range between the first (p) and second (Q) critical end points. In this region, the density of the fluid phase changes with pressure but there is no separation of fluid into liquid and gas at any pressure. The most "low solubility" compounds with relatively high melting temperatures, such as quartz, heavy and alkali earth metals oxides, sulfides, carbonates, silicates and aluminosilicates serve as nonvolatile component in the systems of the second type. Some aqueous systems with "high solubility" compounds such as alkali metal sulfates and carbonates, NaF,  $\text{BaCl}_2$ ,  $\text{Na}_3\text{PO}_4$ , etc., however, also belong to the type 2.

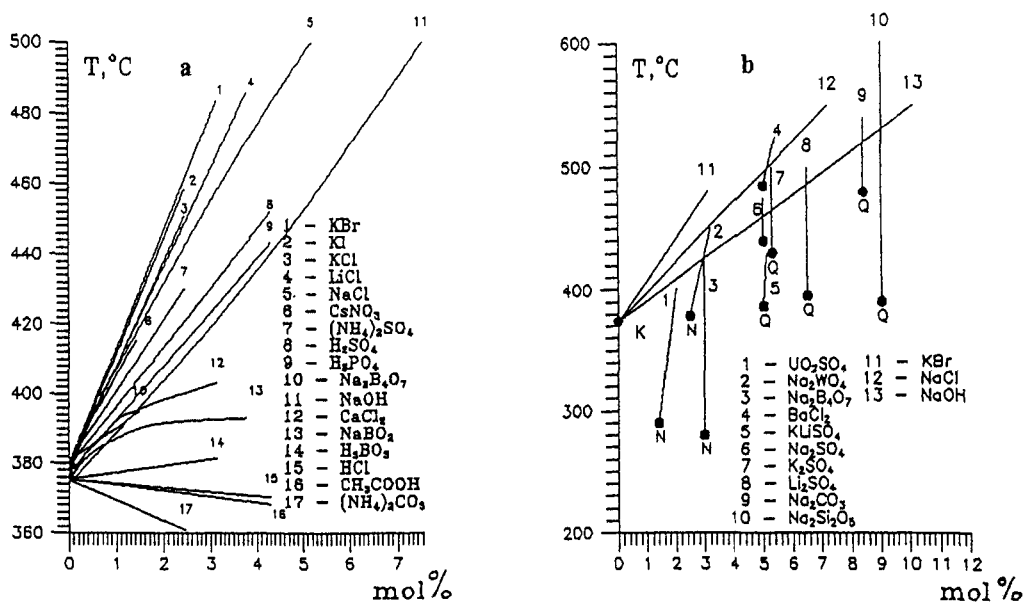


Fig.1 The T-X projections of critical curves for binary water-salt systems [1,5,7,10,16]

a) Liquid-gas critical curves of the first type water-salt systems

b) Liquid-liquid (1-10) and liquid-gas (11-13) critical curves of water-salt systems.

Water-salt systems of both types could be complicated by the immiscibility phenomena which were found at a temperatures higher than 200° C. In systems of the first type, a stable three-phase immiscibility region ( $L_1$ - $L_2$ -G) occurs, whereas in systems of the second type this three-phase immiscibility region is usually metastable. Only the system  $\text{BaCl}_2$ - $\text{H}_2\text{O}$ , attributed to the type 2, has a stable part of three-phase immiscibility region [1,2]. It is important that metastable immiscibility regions were found in all water-salt systems of the second type studied in detail.

The two main types of immiscibility region were distinguished in our classification of binary complete phase diagrams [1-3]. The b-type, corresponding to the types II and VI in the classification of Scott and Koninenburg [8], is characterized by a limited immiscibility region. In this region the equilibrium  $L_1$ - $L_2$

is terminated either by critical phenomena  $L_1=L_2$  and the critical end point N ( $L_1=L_2-G$ ) or by the interactions with solid phase, and does not show a continuous transition into equilibrium L-G. The critical curves  $L_1=L_2$  and  $L=G$  never intersect. The types II and VI [8] arise as versions of the main b-type as a result of immiscibility region interactions with the surfaces of crystallization and are designated as 1b, 1b' [1,3] and 1b<sub>1</sub>, 1b<sub>2</sub>, 1b<sub>1</sub>' [1,2] in our classification.

The c-type (corresponding to the types III and V in [8]) is distinguished by another critical end point R ( $L_1=G-L_2$ ) terminating the three-phase immiscibility region and by continuous transition of  $L_1-L_2$  equilibrium into L-G one. The types III and V [8] arise due to the interaction of the equilibrium  $L_1-L_2$  with solid phase and are referred to as 1c, 1c' [1,3] and 1c<sub>1</sub>, 1c<sub>2</sub>, 1c<sub>1</sub>' [1,2] in our classification.

The type IV [8] shows two immiscibility regions of b- and c-types in a system. The theoretical derivation of fluid phase diagrams [9] produces even more complicated versions of diagrams, with three separate immiscibility regions. However, each of them belongs to one of the main types mentioned above.

Figure 1b illustrates the different behavior of critical curves corresponding to equilibria  $L=G$  and  $L_1=L_2$ . The first curves emerge from the critical point of water, whereas the critical curves  $L_1=L_2$  start in the critical end point N ( $L_1=L_2-G$ ) or Q ( $L_1=L_2-S$ ) depending on the type of the binary system.

## TERNARY SYSTEMS

### IMMISCIBILITY AND CRITICAL PHENOMENA.

In ternary systems, the critical surfaces join the critical curves of the boundary binary systems and inherit the forms of these curves. The simple smooth critical surfaces arise if the critical curves with the same equilibrium are joined. The P-X, P-T and T-X projections of the critical surface  $L_1=L_2$ , joined the same boundary critical lines in the system  $\text{SiO}_2\text{-NaOH-H}_2\text{O}$  [10], are shown as a characteristic example in Fig.2.

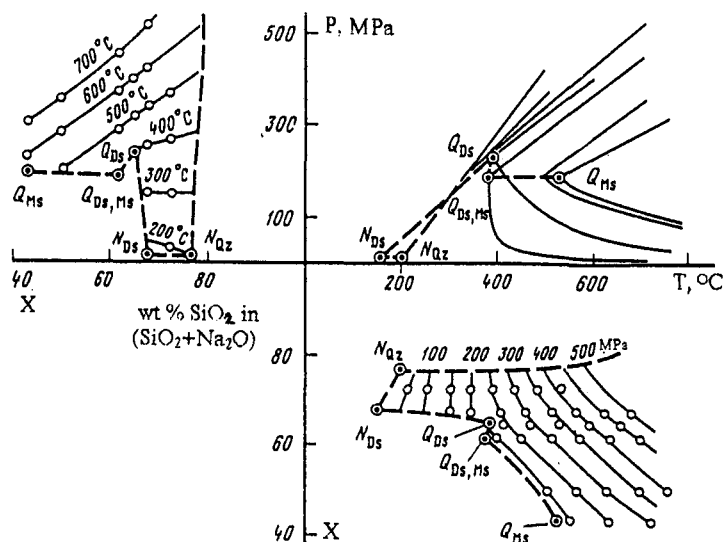


Fig.2 The P-X, P-T and T-X projections of the critical surface  $L_1=L_2$  and mono-variant critical curves of the system  $\text{Na}_2\text{O} - \text{SiO}_2 - \text{H}_2\text{O}$  [10].

Ternary critical curves  $Q_{MS}$ - $Q_{MS,DS}$ ,  $Q_{MS,DS}$ - $Q_{DS}$ ,  $Q_{DS}$ - $N_{DS}$ ,  $N_{DS}$ - $N_{QZ}$  and  $N_{QZ}$ - $Q_{QZ}$  correspond to  $L_1=L_2-S_{MS}$ ,  $L_1=L_2-S_{DS}$ ,  $L_1=L_2-G$ ,  $L_1=L_2-S_{QZ}$  equilibria respectively; MS -  $\text{Na}_2\text{SiO}_3$ ; DS -  $\text{Na}_2\text{Si}_2\text{O}_5$ ; QZ -  $\text{SiO}_2$ .

The form of critical surfaces originating in the critical curves with different phase equilibria is much more complicated and complex than in the case when the critical equilibrium is uniform throughout a critical surface. There are two possibilities shown on the scheme of T-X projection of a ternary phase diagram where both boundary systems with volatile component (A) belong to the first type complicated by the immiscibility regions of different types (Fig.3).

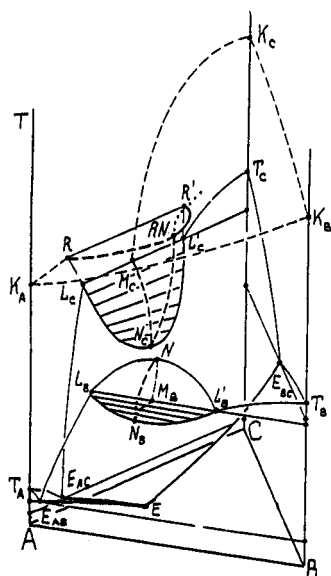


Fig.3 The T-X projection of the complete phase diagram for the ternary system A-B-C with the two boundary systems of the first type complicated by liquid immiscibility regions of the b-type (system A-B) and c-type (system A-C).

Points  $T_A, T_B, T_C$  and  $K_A, K_B, K_C$  are triple and critical points of pure components;  $E_{AC}, E_{AB}, E_{BC}, N, R, M_C, L_C, L_B, M_B$  - invariant points of binary systems, corresponding to the equilibria L-G- $S_1$ - $S_2$ ,  $L_1=G-L_2$ ,  $L_1=L_2-S$ ,  $L_1-L_2-G-S$ ,  $L_1=L_2-G$ ;  $E, LN_C, LN_B, NR$  are invariant points of the ternary system with equilibria L-G- $S_A$ - $S_B$ - $S_C$ ,  $L_1=L_2-G-S$ ,  $L_1=L_2=G$ .

Compositions of liquid phases in monovariant equilibria are shown by solid lines. Compositions of critical fluids in monovariant equilibria are shown by dashed lines.

Compositions of equilibrium vapor phases are not shown for figure simplification.

The b-type immiscibility region occurs in the system A-B and the c-type - in the A-C system. In both systems the three-phase immiscibility region ( $L_1-L_2-G$ ) intersects the three-phase solubility equilibrium (L-G-S) and forms the invariant point L with equilibrium  $L_1-L_2-G-S$ .

The critical surface  $L_1=L_2$ , started in the critical curve N-M of the binary system A-B, does not intersect the critical surface  $L=G$ , originated in the critical line  $K_A-K_B$ . In this case, the different critical equilibria do not interact.

In the case of the interaction of different critical surfaces, a new type of phase equilibria arises. It is so called "the critical phenomena of second order" or "the tricritical point" [11]. The theoretical possibility of equilibrium, at which three coexisting fluid phases simultaneously become identical, was pointed out by Ph.Kohnstamm in 1926 [12]. The first experimental evidence of that phenomenon was found in organic and water-organic systems by two Russian groups in 1962-1963 [13,14].

The tricritical point RN ( $L_1=L_2=G$ ), as shown in Fig.3, arises at the intersection of the two ternary monovariant critical curves R-RN ( $L_1=G-L_2$ ) and  $N_C$ -RN ( $L_1=L_2-G$ ). This point corresponds to a disappearance of the three-phase immiscibility region in ternary mixtures and forms a two-leaf critical surface, which connects the different critical curves  $K_A-K_B$  ( $L=G$ ),  $K_A-R$  ( $L=G$ ),  $K_B-K_C$  ( $L=G$ ) and  $K_C-M$  ( $L_1=L_2, L=G$ ) in the boundary systems.

It is clear from fig.3, that tricritical phenomena should arise in ternary mixtures even though the system A-B belongs to the first type, without immiscibility region. Hence, the main condition of the tricritical equilibrium occurrence in a ternary system is the existence of the c-type immiscibility region in the boundary binary mixtures, which disappears when we add the third component.

We have studied experimentally both types of ternary water-salt systems (with and without the immiscibility region of b-type in one of binary water-salt systems) and have found direct evidence for existence of a tricritical point in both cases.

### TRICRITICAL PHENOMENA IN WATER-SALT SYSTEMS.

**$H_2O$ - $HgI_2$ - $PbI_2$  SYSTEM** Both boundary water-salt systems belong to the type 1, with different types of immiscibility region. Experimental data [15] show that immiscibility region in the system  $H_2O$ - $HgI_2$  (as well as in the system A-B on fig.3) is bounded at high temperatures by the critical end point N ( $L_1=L_2-G$ ) and belongs to the b-type [15]. The three-phase immiscibility equilibrium  $L_1-L_2-G$ , terminating in the critical end point R ( $L_1=G-L_2$ ) in the system  $H_2O$ - $PbI_2$  (as well as in the system A-C in fig.3), belongs to the c-type.

The method of visual observation of phase transformation in a sealed thick-walled quartz tube have been used for investigation of salt solubility, liquid-liquid immiscibility and critical phenomena in the ternary water-salt mixtures [15].

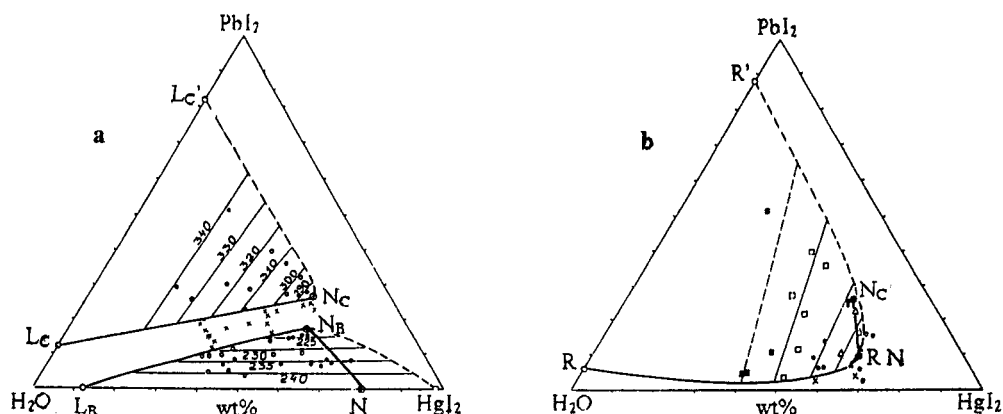


Fig.4 Ternary phase diagrams of the system  $\text{H}_2\text{O}-\text{HgI}_2-\text{PbI}_2$  at high temperatures and vapor pressures [15].

a) Compositions of coexisting liquid phases saturated with solid in the two separated immiscibility regions.

The circles show the compositions where the dissolution of solid was accompanied by liquid-liquid immiscibility. The crosses show the compositions where the solid was dissolved with the production of homogeneous liquid phase. The compositions of concentrated liquid solutions were estimated very roughly and shown by dashed line.

b) compositions of critical fluids (curves  $R-\text{RN}$  and  $N_c-\text{RN}$ ), equilibrium non-critical liquid phase (curve  $R'-\text{RN}$ ), and tricritical point ( $\text{RN}$ ).

The squares, points and triangles show the compositions where the critical phenomena between vapor and dilute liquid solution in equilibrium with concentrated one ( $L_1=G-L_2$ ) were observed. The crosses and circles show the compositions where the liquid immiscibility was absent and critical phenomena  $L=G$  were observed (crosses) or were not reached in experimental conditions (circles). The designations of invariant points are the same as in Fig.3.

The experimental results are represented in fig.4. Figure 4a shows the compositions of two coexisting liquid phases in equilibrium with solid and vapor phases in the two separate immiscibility regions adjacent to the boundary systems  $\text{H}_2\text{O}-\text{PbI}_2$  and  $\text{H}_2\text{O}-\text{HgI}_2$ . The compositions of diluted and concentrated saturated liquids, joined by isothermal tie-lines, approach each other upon decreasing of temperature and increasing concentration of the second salt. The critical phenomena between the two liquids in equilibrium with the vapor and the corresponding solid phase occur at ternary critical end points  $N_c$  ( $L_1=L_2-G-S_{\text{PbI}_2}$ ) and  $N_B$  ( $L_1=L_2-G-S_{\text{HgI}_2}$ ). The last one ( $N_B$ ) is joined with critical end point  $N$  ( $L_1=L_2-G$ ) in the system  $\text{H}_2\text{O}-\text{HgI}_2$  by the monovariant critical curve  $N_B-N$  ( $L_1=L_2-G$ ).

To locate the tricritical point, monovariant critical curves  $L_1=G-L_2$  and  $L_1=L_2-G$  were studied. The first one originates at the binary critical end point  $R$  ( $L_1=G-L_2$ ). The second critical curve originates at the ternary critical end point  $N_c$  ( $L_1=L_2-G$ ). Figure 4b shows the intersection of these curves ( $R-\text{RN}$  and  $N_c-\text{RN}$ ) in the tricritical point  $\text{RN}$ , the isothermal tie-lines between the compositions of the critical solutions ( $R-\text{RN}$ ) and the equilibrium liquid phase ( $R'-\text{RN}$ ).

The parameters of the tricritical point  $\text{RN}$  are the following:  $401 \pm 1^\circ \text{C}$ ;  $1.4 \pm 0.1 \text{ mol}\%$   $\text{PbI}_2$  and  $9.2 \pm 0.2 \text{ mol}\%$   $\text{HgI}_2$ .

***H<sub>2</sub>O-NaCl-Na<sub>2</sub>B<sub>4</sub>O<sub>7</sub> SYSTEM*** In this ternary system the immiscibility region of c-type, terminated by the lower (N ( $L_1=L_2-G$ )) and upper (R ( $L_1=G-L_2$ )) critical end points, occurs in the system  $H_2O-Na_2B_4O_7$  [16].

The phase behavior in the ternary system  $H_2O-NaCl-Na_2B_4O_7$  was studied by vapor pressure measurements of the mixtures with constant salt-to-salt ratios (15, 25, 35, 50 mol% NaCl in the NaCl+ $Na_2B_4O_7$  mixtures) and varying content of water. The temperature was held constant at 388, 400, 405 and 410° C [17].

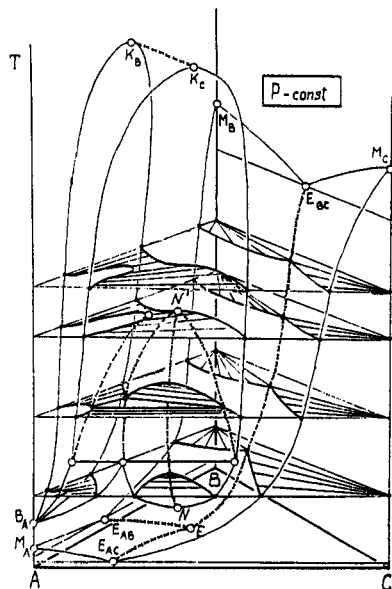


Fig.5 The ternary prism of isobaric T-X cross-section of the complete phase diagram for ternary system A-B-C with the first type boundary system A-C complicated by liquid immiscibility region of the c-type.

Points  $M_A, M_B, M_C$  and  $B_A$  are melting and boiling points of pure components;  $E_{AB}, E_{BC}, E_{AC}$  and  $E$  show compositions of the liquids in equilibrium with two and three solid phases;  $N, N'$  - compositions of the critical fluids. Solid lines show compositions of equilibrium liquid and gas solutions, dashed lines-compositions of solutions in ternary monovariant equilibria. Triangular sections of the prism show all the equilibria in ternary mixtures at constant T, P.

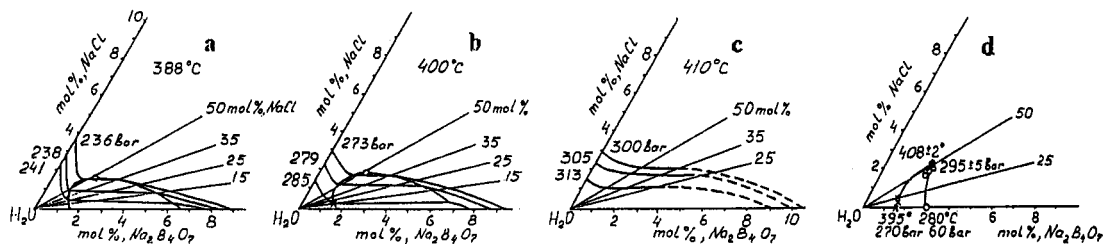


Fig.6 Ternary phase diagrams of the system  $H_2O-Na_2B_4O_7-NaCl$  at high temperatures and vapor pressures [17].

a-c) Compositions of the liquid solutions in two-phase (L-G) and three-phase (L<sub>1</sub>-L<sub>2</sub>-G) equilibria at constant pressures and temperatures 388 (a), 400 (b) and 410° C (c).

d) Compositions of two ternary critical curves, meeting at the tricritical point.

The isobaric cross-section of the ternary phase diagram (fig. 5) shows that the three-phase immiscibility region (L<sub>1</sub>-L<sub>2</sub>-G) disappears with increases in temperature and second salt (B) concentration. Theoretical derivation of such isobaric or isothermal schemes as well as the projections of the complete phase diagram (such as shown in fig.3) has the objective of obtaining insight into the most appropriate choice of experimental method and strategy of investigation, allowing better interpretation of the experimental data. In this instance the isobaric cross-section in fig.5 shows both the ternary diagrams at constant temperature and pressure, and their transformation with temperature. Such information permits not only to determination of the borders of immiscibility region from the experimental data, but also estimation of the parameters of the lower ( $L_1=L_2-G$ ) and upper ( $L_1=G-L_2$ )

critical points for ternary mixtures. These critical points are joined by two monovariant critical curves, which meet at the tricritical point.

Figure 6(a-c) shows the compositions of homogeneous liquid and immiscible liquid phases in equilibrium with vapor at constant temperatures and pressures. Also shown are the compositions of supercritical and critical fluids, obtained by interpolation of experimental data. The extent of the ternary critical curves, starting in the binary critical end points N and R, is demonstrated in fig.6d.

The difference in critical parameters of these curves should vanish at the tricritical point. Short extrapolation of the experimental data gives a range of temperature, pressure and composition, where the tricritical phenomena occur. The tricritical parameters for the system  $\text{H}_2\text{O}-\text{NaCl}-\text{Na}_2\text{B}_4\text{O}_7$ , evaluated in this way, are the following :  $408 \pm 2^\circ \text{C}$ ;  $295 \pm 5$  bars;  $2.2 \pm 0.2$  mol% NaCl;  $2.2 \pm 0.2$  mol%  $\text{Na}_2\text{B}_4\text{O}_7$ .

## SOLUBILITY PHENOMENA IN HYDROTHERMAL CONDITIONS

So far, the phase behavior in ternary water-salt systems has been discussed for the cases where both boundary water-salt systems belong to the type 1. In these cases, the usual shape of solubility surfaces for the three-phase equilibrium (L-G-S), with singular minima at eutonic and eutectic compositions can be complicated by an immiscibility phenomena as shown in fig.3.

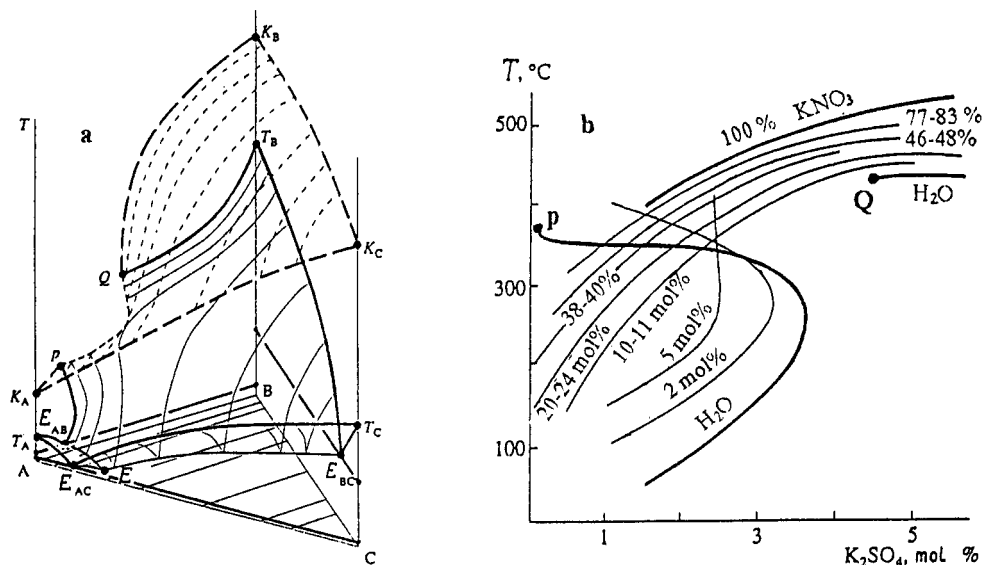


Fig.7 The T-X projections of phase diagrams for the ternary systems with one boundary system of the type 2 (A-B,  $\text{H}_2\text{O}-\text{K}_2\text{SO}_4$ ) and the other - of the type 1.

a) ternary prism of the complete phase diagram for the system A-B-C.

The designations are the same as in Fig.4. Thin dashed and solid lines show the cross-sections of critical and solubility surfaces at constant contents of the component C.

b) temperature dependence of  $\text{K}_2\text{SO}_4$  solubility in the system  $\text{H}_2\text{O}-\text{K}_2\text{SO}_4-\text{KNO}_3$  at vapor pressures and constant concentrations of  $\text{KNO}_3$  (from 0 ( $\text{H}_2\text{O}$ ) up to 100 %) [19].

If one of the boundary binary water-salt systems belongs to the type 2, new phenomena in solubility behavior in the ternary systems are observed. The addition a salt of the first type to binary mixtures of the second type results in the following:

- the sign of t.c.s. changes from negative to positive,
- supercritical fluid equilibria and critical phenomena in ternary solutions saturated with the second type salt should disappear,

- the metastable immiscibility region spreads from the second type boundary system into the ternary one and disappears in metastable conditions or after transformation into stable equilibria.

All ternary hydrothermal systems of this type, studied up to now, exhibit the disappearance of the three-phase immiscibility region only under metastable conditions. However, the specific shape of stable ternary solubility surface in a region adjacent to the second type boundary system gives the evidence of the metastable immiscibility spreading into the supersaturated three-component region [1,18].

The P-X projection of the complete phase diagram for the ternary system with the boundary systems of type 1 (A-C and B-C) and type 2 (A-B) is given in fig.7a. The monovariant critical curve p-Q, corresponding to the intersection of critical ( $K_A$ -p-Q- $K_B$ - $K_C$ ) and solubility ( $E_{AB}$ -p-Q- $T_B$ - $E_{BC}$ -E) surfaces, bounds the supercritical fluid equilibria region in the ternary system. It is felt that the concentration of B is rather low in the critical solutions saturated with the solid C (curve p-Q). However, the experimental data for this critical equilibrium in such ternary water-salt systems are not yet available. The data, obtained for such hydrothermal systems, are usually limited by salt solubility measurements.

An example of the solubility behavior of the second type salt in hydrothermal solutions of the first type electrolyte is demonstrated in fig.7b. The solubility surface of  $K_2SO_4$  is represented by a set of isopleths with near constant contents of  $KNO_3$ . The temperature dependence of  $K_2SO_4$  solubility changes with increasing of  $KNO_3$  concentration. A negative t.c.s of  $K_2SO_4$  in water and dilute  $KNO_3$  solutions becomes a positive when the general concentration of saturated solution reaches 7-7.5 mol % [19].

In a region where the sign of t.c.s changes, the most drastic transformations of the solution structure are expected. Indeed, this region is distinguished by fundamental change in behavior of thermodynamic, transport and spectroscopic properties from "waterlike" to "meltlike" (such as t.c.s.) [1,3]. Another peculiarities of the transition region are the appearance of the liquid-liquid immiscibility in such hydrothermal electrolyte solutions and the systematic decrease of transition concentration with an increase of ionic charge in solutions [1].

## ANALYTICAL DESCRIPTION OF HYDROTHERMAL SOLUBILITY.

There are several approaches for thermodynamic calculation of salt solubility at high temperatures and pressures [20-26]. One of them developed by Lietzke, Stoughton [24], Marshall [25] and Malinin [26] shows that solubility of the second type "low solubility" compounds such as  $CaSO_4$ ,  $BaSO_4$ ,  $Ag_2SO_4$ ,  $CaF_2$ ,  $CaMoO_4$ , etc. in hydrothermal electrolyte solutions of ionic strength up to 2-3 m, could be conveniently described by extended Debye-Huckel theory using the equation

$$\log Q_{sp} = \log K_{sp} + \sum z^2 \cdot S \cdot \sqrt{I} / (1 + A \cdot \sqrt{I}) \quad (1)$$

where  $Q_{sp}$  and  $K_{sp}$  are the solubility and activity products of dissolved salt,  $z$  is the charge of ions,  $S$  is the theoretical Debye-Huckel limiting slope,  $I$  is the ionic strength of solution, and  $A$  is the parameter related to the ion size.

We have checked the adherence of that approach for the second type "high solubility" compounds such as  $Na_2SO_4$ ,  $Na_2CO_3$  and  $K_2SO_4$ , using the available experimental data on the solubility of these compounds in NaOH-, NaCl-, KCl- and  $KNO_3$ -bearing hydrothermal solutions [5,18,19,27]. The calculation of the solubility products has been done for a wide range of concentrations up to the ionic strength of several tens molality which is higher than the transition concentrations for these systems [28].

The linear dependence of solubility product on the ionic strength with a theoretical slope is confirmed up to extremely high concentrations of the solutions (see fig.8). Moreover, the careful analysis of the data shows that the systematic deviation of the experimental values from the theoretical straight line is observed when the solution concentration exceeds that of the transition region.



It is surprising that such a primitive model, which describes the thermodynamics of aqueous electrolyte solutions only up to 0.2-0.5 m at ambient temperatures, produces good agreement with

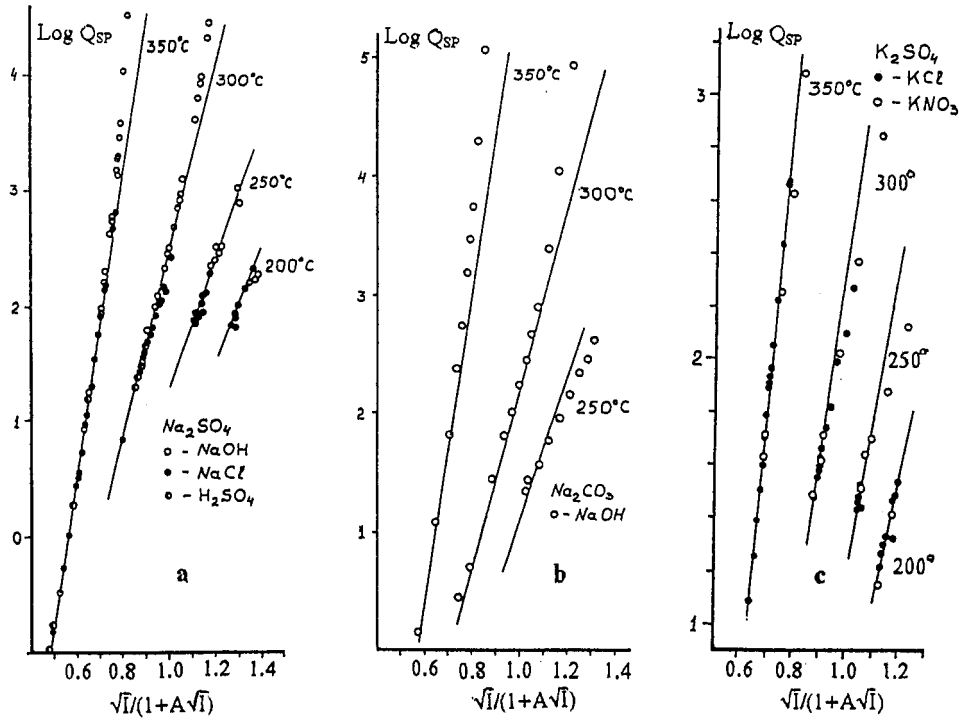


Fig.8 Plots of the logarithm of the solubility products ( $Q_{\text{SP}}$ ) of  $\text{Na}_2\text{SO}_4$  (a),  $\text{Na}_2\text{CO}_3$  (b) and  $\text{K}_2\text{SO}_4$  (c) in aqueous solutions of  $\text{NaOH}$ ,  $\text{NaCl}$ ,  $\text{H}_2\text{SO}_4$ ,  $\text{KCl}$  and  $\text{KNO}_3$  vs a function of the ionic strength at 200-350°C and vapor pressures [5,18,19,27].

The straight lines represent Debye-Huckel theoretical slopes.

experimental data for salt solubility in hydrothermal solutions with the ionic strength up to 2-3 m and even 10-16 m (in the case of "high solubility" salts of type 2).

It was shown [25,26] that this approach is largely sensitive to the processes of association, hydrolysis and other chemical interactions in aqueous solutions, which produce new molecular species. However, the quantitative agreement between experimental and calculated data on solubility demonstrates that interactions between the ions and other particles are not significantly detectable.

If the obtained results are not coincidental and the effects which were not taken into account by the Debye-Huckel model, compensate each other and are eliminated by correctly described processes of ion interaction in hydrothermal solutions, the following conclusions can be drawn.

The processes of association and other above-mentioned factors are absent in the given solution up to high electrolyte concentrations.

The equation (1) provides the correct description of the hydrothermal solubility in a wide range of electrolyte concentration in the case of the general increase of ion-ion interactions in the hydrothermal solutions with "waterlike" structure, if the process of formation of the new molecular species is not taking place.

The hydrothermal solutions with electrolyte concentrations above the transition region are distinguished by a different molecular structure with "meltlike" network of ionic bonds. The new system of molecular interactions can not be described by the Debye-Huckel model and gives rise to the discrepancy between the calculated and experimental values of the hydrothermal solubility.

## REFERENCES

1. V.M.Valyashko. *Phase Equilibria and Properties of Hydrothermal Solutions*, Nauka, Moscow, 270 p. (1990).
2. V.M.Valyashko. *Z.Phys.Chem.*, **267**, 481-493 (1986).
3. V.M.Valyashko. *Pure & Appl.Chem.*, **62**, 2129-2138 (1990); **67**, 569-578 (1995).
4. G.M.Schneider. *Adv.Chem.Phys.*, **17**, 1-42 (1970); *Pure & Appl.Chem.*, **47**, 277-291 (1976); **65**, 173-182 (1993).
5. M.I.Ravich. *Water-Salt Systems at Elevated Temperatures and Pressures*, Nauka, Moscow, 150 p.(1974).
6. B.C.-Y.Lu and D.Zhang. *Pure & Appl.Chem.*, **61**, 1065-1074 (1989).
7. W.L.Marshall and E.V.Jones. *J.inorg.nucl.Chem.*, **36**, 2313-2318 (1974).
8. R.L. Scott and P.N. Van Konynenburg. *Disc.Farad.Soc.*, **49**, 87-97 (1970); *Phil.Trans.Roy.Soc.(London)*, **298A**, 495-540 (1980)
9. L.Z.Boshkov. *Dokl.AN SSSR*, **294**, 901-905 (1987)
10. V.M.Valyashko, K.G.Kravchuk. *Dokl.AN SSSR*, **242**, 1104-1107 (1978)
11. R.B.Griffiths, *J.Chem.Phys.*, **60**, 195-206 (1974)
12. Ph.Kohnstamm. in *Handbuch der Physik*, edited by H.Geiger, K.Scheel, Spinger, Berlin, **10**, p.223 (1926).
13. I.R.Krichevskii, G.D.Efremova, A.V.Shvarts et al. *Zh.Fiz.Khim.*, **37**, 1924-1929 (1963); **40**, 907-911 (1966); *Ukrain.Fiz.Zh.*, **9**, 481-494 (1964).
14. G.S. Radshevskaya, N.I.Nikurashina, R.V. Mertslin et al. *Zh.Obshch.Khim.*, **32**, 673-681 (1962); *Zh.Fiz.Khim.*, **43**, 416-421 (1969); **45**, 797-784 (1971).
15. V.M.Valyashko and M.A.Urusova. *Zh.Neorgan.Khim.*, **41**, 1355-1369 (1996).
16. M.A. Urusova and V.M.Valyashko. *Zh.Neorg.Khim.*, **35**, 1273-1279 (1990).
17. M.A. Urusova and V.M.Valyashko. *Zh.Neorg.Khim.*, in press.
18. V.M.Valyashko, *Zh.Neorg.Khim.*, **18**, 1114-1118 (1973).
19. Kh.Ataev, V.M. Valyashko, K.G.Kravchuk et al. *Zh.Neorg.Khim.*, **39**, 523-528 (1994).
20. H.C. Helgeson and D.H. Kirkham. *Amer.J.Sci.*, **277**, 1089-1261 (1974); **276**, 97-240 (1976).
21. *Activity Coefficients in Electrolyte Solutions*. Editor K.S.Pitzer, CRC Press, 2nd Edition (1991).
22. R.J.Fernandez-Prini, H.R. Corti and M.L. Japas. *High-Temperature Aqueous Solutions: Thermodynamic Properties*, CRC Press, 207 p. (1992).
23. V.I. Zarembo and L.V. Puchkov. *Obzori po Teplofiz.Svoystv.Veshchestv*, IVTAN, Moscow, N 2(46), 106 p. (1984).
24. R.W. Stoughton and M.V. Lietzke. *J.Phys.Chem.*, **64**, 113, 816, 1445 (1960); **67**, 652 (1963).
25. W.L. Marshall. *Rev.Pure & Appl.Chem.*, **18**, 167 (1968); *J.inorg.nucl.Chem.*, **37**, 1191-1202, 2155-2163 (1975); *Pure & Appl.Chem.*, **57**, 283-301 (1985)
26. S.D. Malinin. *Physical Chemistry of Hydrothermal Solutions with CO<sub>2</sub>*, Nauka, Moscow, 110 p. (1979).
27. W.C. Schroeder, A. Gabriel, A.A. Berk et al. *J.Amer.Chem.Soc.*, **57**, 1539-1546 (1935); **58**, 843-849 (1936); **59**, 1783-1790 (1937).
28. V.M.Valyashko, Kh.Ataev and P.Yu. Aleshko-Ozhevsky. Dep.VINITI, Moscow, IONKh RAN, N 2610-B96, 38 p., 06.08.1996.